NANO LETTERS
2006
Vol. 6, No. 4
699−703

Atomic Layer Deposition on Suspended Single-Walled Carbon Nanotubes via Gas-Phase Noncovalent Functionalization

Damon B. Farmer[†] and Roy G. Gordon*[,‡]

Division of Engineering and Applied Sciences and Department of Chemistry and Chemical Biology, Harvard University, Cambridge, Massachusetts 02138

Received December 12, 2005; Revised Manuscript Received February 6, 2006

ABSTRACT

Alternating exposures of nitrogen dioxide gas and trimethylaluminum vapor are shown to functionalize the surfaces of single-walled carbon nanotubes with a self-limited monolayer. Functionalized nanotube surfaces are susceptible to atomic layer deposition of continuous, radially isotropic material. This allows for the creation of coaxial nanotube structures of multiple materials with precisely controlled diameters. Functionalization involves only weak physical bonding, avoiding covalent modification, which should preserve the unique optical, electrical, and mechanical properties of the nanotubes.

Atomic layer deposition (ALD) on single-walled carbon nanotubes (SWNTs) is of interest for many reasons. In particular, ALD of high-κ dielectric materials has been shown to produce a benign dielectric/SWNT interface that does not adversely affect the electrical properties of the nanotube.[1] Combining this fact with the low-temperature processing and subnanometer thickness precision that is inherent to ALD makes it an ideal deposition technique for nondestructively passivating SWNTs with very thin, high-κ materials. Coaxial coating is particularly desirable because its realization makes coaxially gated SWNT devices feasible. This configuration would maximize the capacitive coupling of the nanotube with its gate, which is a crucial step toward optimizing the device characteristics.[2,3] Furthermore, it has been suggested that a suspended SWNT geometry may be necessary to satisfy scalability requirements for future devices.[4] Such a structure would necessitate coaxial insulation.

The problem in using ALD for this purpose is that the SWNT surface is chemically inert to ALD precursor molecules, which eliminates the possibility of direct deposition.[1] Previous work that employed ALD to passivate SWNTs utilized substrate-assisted growth, where dielectrics grown on a supporting substrate encased the nanotube.[5] This constraint severely limits device design and makes the fabrication of radially isotropic coatings impossible. It is therefore desirable to establish functionalization techniques that make SWNTs susceptible to ALD precursors. Previously, we described a liquid-based technique that functionalizes SWNTs through covalent chemical bonding.[6] Although this technique made SWNTs susceptible to ALD, it is experimentally tedious and may be impractical in large-scale fabrication processes. Furthermore, chemical functionalization changes the hybridization state of the nanotubes, destroying their unique optoelectronic properties.[7,8] As a result, postfunctionalization heat treatments are needed to recover the initial hybridization state. Here, we describe a simpler technique using nitrogen dioxide (NO_2) gas and trimethylaluminum (TMA, $Al[CH_3]_3$) vapor that functionalizes SWNTs through a less destructive physical interaction.

Functionalization was studied by probing the electrical conductance of SWNTs during the functionalization procedure, and the resulting ALD coating behavior was examined by transmission electron microscopy (TEM). Samples for electrical analysis were fabricated using optical lithography and electron beam evaporation techniques to pattern metal electrodes (50 nm Mo/50 nm Ti) on quartz substrates. The electrodes were separated by trenches (1 μm wide, 0.5 μm deep) that were fabricated using a focused ion beam (FIB). Approximately 0.5 nm of ALD aluminum oxide (Al_2O_3)[9,10] was deposited on the electrode surfaces to prevent alloying between the molybdenum and the nanotube catalyst metal, which was ~0.3 nm of ALD cobalt (Co).[11] SWNT synthesis was carried out at atmospheric pressure by bubbling argon (~450 sccm) through ethanol and flowing the mixture over the samples at high temperatures (750−900 °C) in an Inconel

* Corresponding author. E-mail: gordon@chemistry.harvard.edu.
† Division of Engineering and Applied Sciences.
‡ Department of Chemistry and Chemical Biology.

10.1021/nl052453d CCC: $33.50 © 2006 American Chemical Society
Published on Web 03/04/2006

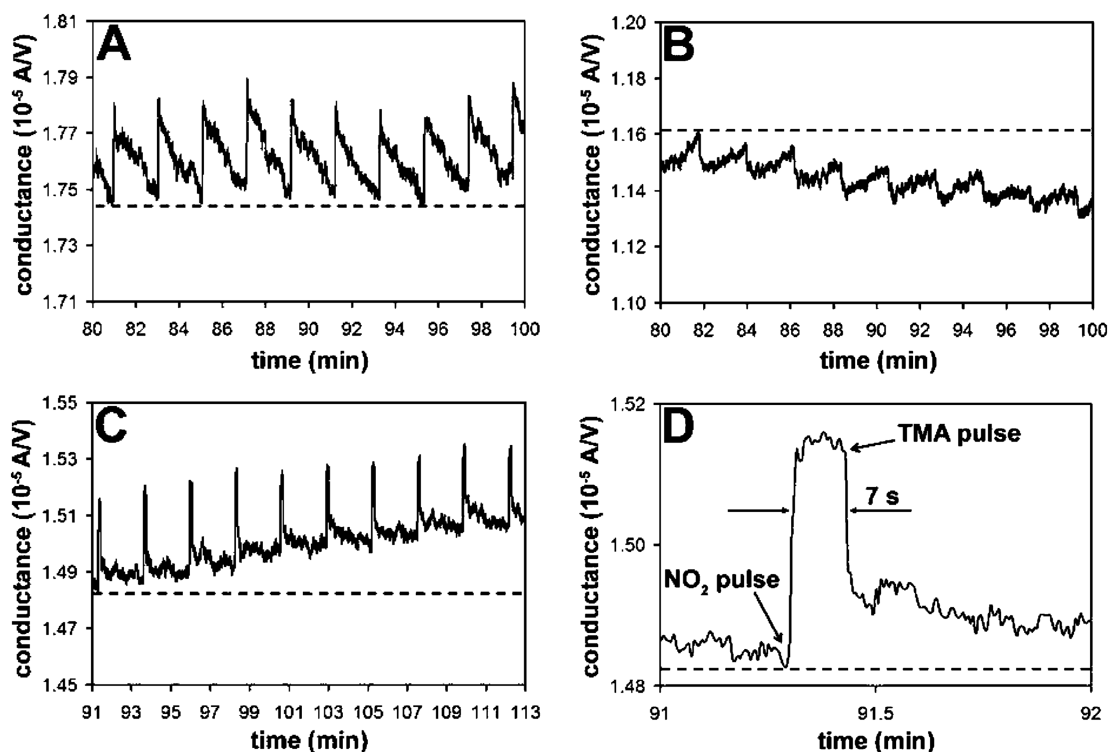

Figure 1. Electrical response of a suspended SWNT sample upon gas exposure. The time between each exposure is 2 min. (A) NO_2 dosing (pulse 40−49, zero slope). (B) TMA dosing (pulse 40−49, negative slope). (C) NO_2-TMA functionalization (cycle 40−49, positive slope). (D) One NO_2-TMA cycle showing the peak shape and time between NO_2 and TMA exposure.

tube (1.35 in ID, ∼860 mL).[12] Growth times varied between 30 s and 5 min. During the synthesis, SWNTs became electrically accessible by growing between the electrodes, over the trench. Semiconducting SWNTs grown in this way exhibit p-type behavior.[13] For the TEM studies, the FIB was used to mill holes into 200-nm-thick silicon nitride membranes. ALD Co was then deposited onto the nitride surface, and nanotube synthesis was carried out as outlined above. During growth, SWNTs grew over the holes, making their suspended sections ideal for TEM analysis.

In our experimental setup, SWNTs can be grown, functionalized, and deposited with ALD material in the same reactor. The suspended SWNT samples can therefore be kept in a controlled vacuum-sealed environment throughout the entire experimental procedure. This eliminates all sources of contamination and ensures that the NO_2-TMA process is directly responsible for the functionalization. The ability to execute every experimental step in one reactor also illustrates the ease with which this functionalization technique can be integrated into a fabrication process.

SWNTs have been used previously as chemical sensors to detect small amounts of NO_2 via strong physical adsorption onto the nanotube sidewalls.[14] In semiconducting SWNTs, adsorption enhances the p-type character through charge transfer of electrons from the tube to the adsorbed NO_2 molecules.[15] This is illustrated in Figure 1a, where ∼30 mL doses of NO_2 at ∼960 Torr are pulsed over suspended SWNTs under steady-state conditions in vacuum (∼300 mTorr, 25 °C). Between each pulse, the NO_2 is purged with a continuous flow of argon (50 sccm) for 2 min. The conductance of the SWNTs increases upon NO_2 exposure, followed by recovery to the initial baseline conductance during the purge, which is indicative of physical desorption. We have found previously that aryl nitrite groups (phenyl-NO_2) react readily with ALD precursors,[6] so it is reasonable to attempt to use adsorbed NO_2 molecules as nucleation sites for ALD. The challenge is to form a continuous monolayer of NO_2 around the suspended SWNTs so that subsequent ALD growth is continuous and uniform over the nanotube surface. Because of desorption, however, this cannot be done with NO_2 alone.

To remedy the desorption problem, we have found that reacting TMA with the adsorbed NO_2 forms a more stable complex that does not desorb from the nanotube sidewalls at room temperature. Evidence for this stabilization comes from the electrical conductance of SWNTs during gas exposures. TMA exposure causes a decrease in SWNT conductance. This can be seen in Figure 1b, where ∼6 mL doses of TMA at ∼10 Torr were pulsed over suspended SWNTs under the same conditions that were used in the NO_2 pulsing. The conductance following TMA exposure recovers slightly because of desorption, but it does not return to a constant baseline value as it did with NO_2 exposure. This results in an overall negative slope in the conductance/time profile, which may be due to an increase in contact resistance at the Mo electrodes caused by the reaction of TMA with surface hydroxyls. When a NO_2 pulse is followed by a TMA pulse, every conductance increase caused by the NO_2 is offset by a conductance decrease caused by the TMA (Figure 1c and d). Recall that when NO_2 is dosed by itself under steady-state conditions the conductance returns to a baseline value and the average slope is zero. This is not the case when NO_2

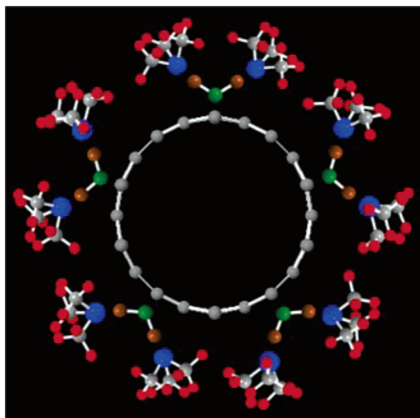

Figure 2. Schematic diagram of the proposed NO_2-TMA functionalization mechanism. NO_2 is adsorbed onto the SWNT surface, and TMA is adsorbed onto the NO_2. This forms a self-terminating monolayer around the nanotube.

dosing is followed by TMA exposure. When this is done, the current rises stepwise with every NO_2-TMA cycle and there is a net positive slope. If NO_2 could freely desorb, then one would expect the slope to be zero as in Figure 1a or even negative because of the presence of TMA. The positive net slope produced by the NO_2-TMA treatment therefore suggests that TMA reacts with NO_2 to inhibit desorption, resulting in a stable complex on the SWNT surface.

A plausible reaction mechanism for adsorbed NO_2 with TMA is illustrated schematically in Figure 2. Here, the nitrogen end of NO_2 is attracted to the SWNT surface, leaving the oxygen ends exposed to incoming TMA vapor. This is the most stable configuration for adsorbed NO_2 molecules on the nanotube surface.[16] The aluminum centers of TMA are in turn attracted to oxygen, leaving the methyl groups ($-CH_3$) as the surface functional groups.[17] These adsorbed NO_2-TMA complexes are substantially larger than adsorbed NO_2. This increase in size can cause an increase in the potential barrier for desorption, and is therefore a likely reason for the observed increase in stability. It will be shown that this configuration results in self-terminating behavior, preventing further attachment of either NO_2 or TMA.

NO_2-TMA functionalization allows for the coating of SWNTs with ALD material, such as high-κ dielectrics. To prove this, suspended SWNTs were exposed to 50 NO_2-TMA cycles in vacuum (~300 mTorr) under the continuous flow of argon (~50 sccm) at 25 °C. A cycle consisted of a NO_2 dose followed by a 7 s purge, then a TMA dose followed by a 2 min purge. After the 50 cycles were complete, 5 cycles (~0.5 nm) of high-κ Al_2O_3 were deposited by ALD at 25 °C in order to further stabilize the functionalization layer. The temperature was then increased to 225 °C for additional Al_2O_3 deposition. TEM micrographs (Figure 3a and b) reveal the resulting ALD coating around SWNTs to be uniform and continuous. The thickness of the oxide layer is 10 nm, which is exactly what was expected for the number of ALD cycles carried out. This means that deposition on the functional layer exhibits little, if any, inhibition or delay in nucleation of ALD Al_2O_3.

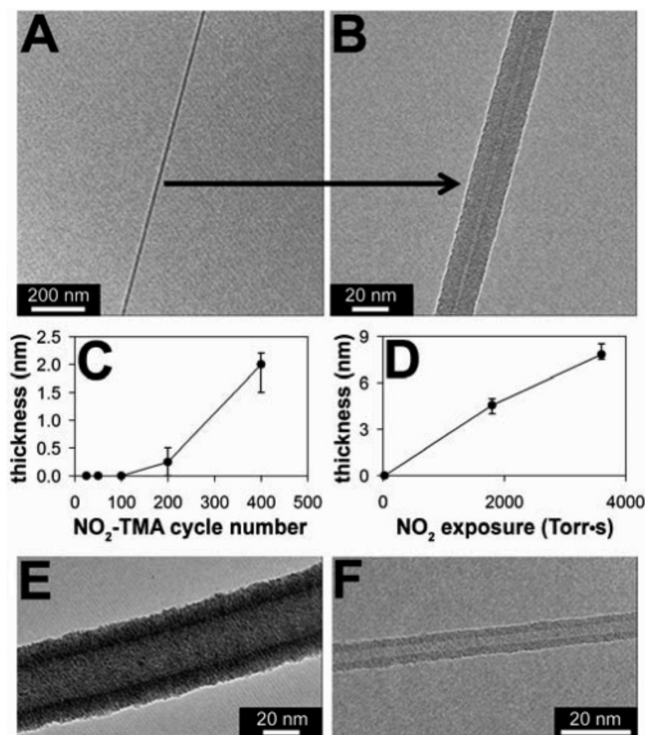

Figure 3. ALD coating behavior of suspended, functionalized SWNTs. (A) TEM micrograph of an Al_2O_3-coated SWNT. (B) Higher magnification of the ~2 nm nanotube reveals the 10 nm coating to be uniform and continuous. (C) Cycle dependence of monolayer breakdown during flow-through-style NO_2-TMA dosing. A multilayer begins to form around 200 functionalization cycles. (D) Higher NO_2 exposures cause the multilayer thickness to increase. (E) A SWNT core−shell structure: 10 nm of ALD Al_2O_3 encased in 10 nm of ALD WN metal. (F) A 2-nm-thick ALD Al_2O_3 layer deposited around a ~3 nm SWNT using optimized functionalization parameters.

Using the same conditions as above but varying the number of NO_2-TMA cycles helps to elucidate the nature of the functional layer. The thickness of this layer remains constant up to 100 NO_2-TMA cycles (Figure 3c). This confirms that the NO_2-TMA technique forms a self-terminating monolayer on the SWNT surface. We speculate that the chemical inertness of the surface methyl groups to NO_2 is the reason that the functionalization is self-limited at a monolayer. Only when both water (H_2O) and TMA are added does the growth continue. Water molecules cleave the methyl groups from their aluminum centers, leaving hydroxyl groups ($-OH$) in their place and methane (CH_4) as a gaseous byproduct. This newly hydroxylated surface is in turn susceptible to ALD reactions with TMA through similar cleavage mechanisms. Alternating exposures of H_2O and TMA in this manner results in ALD Al_2O_3 growth. It is remarkable that the combination of water and TMA allows further growth, whereas the reaction of NO_2 with TMA does not.

When more than 100 NO_2-TMA cycles are carried out, the functional layer does increase in thickness. Imperfections in the methyl surface eventually lead to deterioration of the monolayer, which begins around 200 cycles, and is prevalent by 400 cycles. Breakdown of the self-limiting behavior causes a porous, nonuniform multilayer to form on the

SWNT surface (Figure 3c). The thickness of this layer is directly proportional to the NO_2 exposure, that is, the number of collisions that NO_2 gas molecules can make with the monolayer before they are purged (Figure 3d). More collisions increase the chance of NO_2 molecules finding and adsorbing onto imperfections in the monolayer. NO_2 adsorbed in this way would then act as an adsorption site for incoming TMA. With this happening over many cycles, a multilayer with appreciable thickness can be produced. We therefore optimized the functionalization procedure by using low exposure, flow-through style dosing,[18] and a small number of cycles (<100), as was done in Figure 3a and b.

Dosing 50 cycles of NO_2-TMA followed by 5 cycles of Al_2O_3 ALD at 25 °C sufficiently functionalizes and stabilizes the suspended SWNT surface for ALD at higher temperatures. Most SWNTs treated in this fashion exhibit ideal ALD coating that is uniform and continuous along the entire suspended length of the tube. Utilizing this functionalization technique and the ability to deposit metals and insulators with ALD allows the creation of useful coaxial core−shell structures, such as coaxially gated SWNT field-effect transistors (Figure 3e). Furthermore, the precise thickness control afforded by ALD allows for exceptionally thin, high-κ coatings (Figure 3f). A few unfunctionalized, bare regions have been observed, but their occurrence is sporadic. The five-cycle Al_2O_3 stabilization layer has been found to be necessary because it prevents the NO_2-TMA complexes from migrating or desorbing from the nanotube surface at higher temperatures. Elimination of this stabilization layer results in ALD coating that is radially isotropic but not continuous along the nanotube length, exhibiting many uncoated regions. An identical, negative result was attained by eliminating the five-cycle stabilization step and instead only introducing water vapor over the functionalized nanotubes in the hope of cross-linking the NO_2-TMA complexes. Uncoated sections are also predominant if the functionalization procedure is carried out at conventional ALD temperatures (200−400 °C). Here, the thermal kinetic energy gained by NO_2 molecules causes a decrease in adsorption onto the nanotubes, inhibiting functionalization.

Using optimized functionalization parameters, we explored the effect of the NO_2-TMA treatment on electrical conduction in the nanotubes. As was seen in Figure 1c, the overall effect of functionalization is to cause an increase in conduction. It is important, however, to isolate conduction changes caused by charge-transfer doping of the nanotubes from conduction changes caused by modulation of the Schottky barriers at the contacts between the SWNTs and the Mo electrodes.[19] This is accomplished by utilizing the inertness of SWNTs to selectively passivate the barriers with ALD oxide. Figure 4a shows the effect of a NO_2 dose on an as-grown suspended tube. The exposure causes a conductance increase of $\sim 10^{-5}$ A/V, followed by a decrease due to desorption. After a 12 h purge, the sample was coated with 10 nm of ALD Al_2O_3. This deposition leaves the suspended nanotube exposed, but it coats the Mo/SWNT junction, effectively passivating the Schottky barriers.[6] Figure 4b shows the effect of NO_2 exposure on the same sample after barrier passivation. The

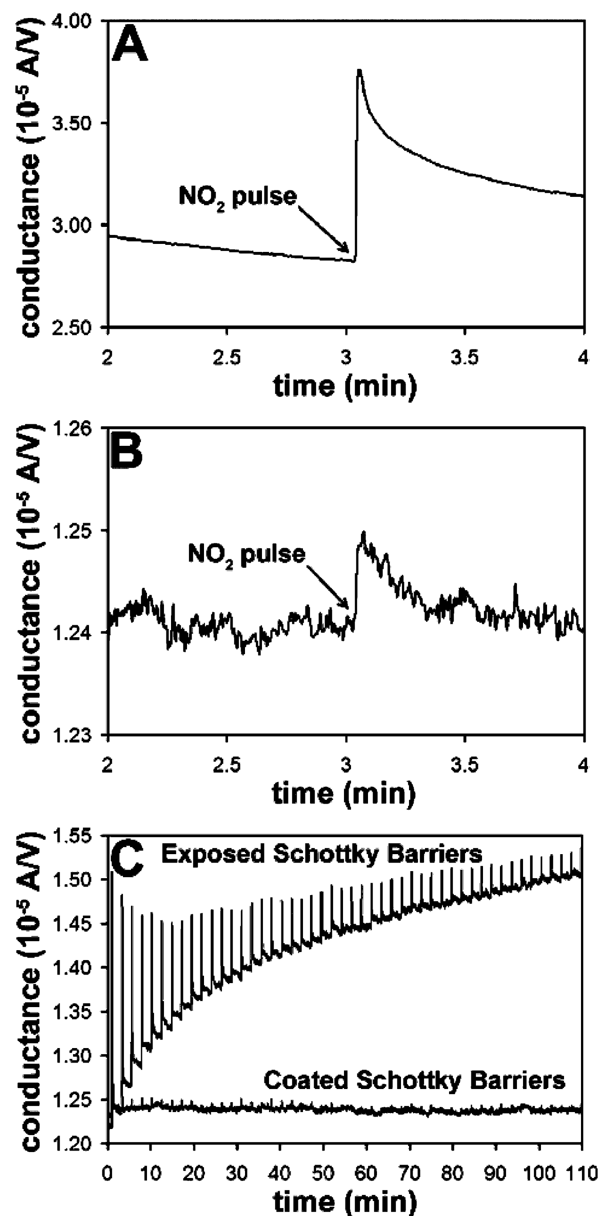

Figure 4. Effect of Schottky barrier passivation on NO_2 exposure and NO_2-TMA functionalization. (A) NO_2 exposure on a suspended SWNT sample with exposed barriers. (B) NO_2 exposure on the same sample with coated barriers. (C) Functionalization cycles on a suspended SWNT sample with exposed barriers compared to a sample with coated barriers.

conductance increase is now only $\sim 10^{-7}$ A/V, 2 orders of magnitude smaller than it was with the exposed barriers. From this we conclude that most of the conductance change caused by NO_2 occurs through modulation of the Schottky barriers. Further illustration of this is seen during the NO_2-TMA treatment. In Figure 4c, a suspended SWNT sample with exposed Schottky barriers is compared to a sample with coated barriers. Both samples were exposed to 50 NO_2-TMA cycles. The conductance of the exposed sample changes significantly while the conductance of the coated sample is relatively constant. These results show that Schottky barrier modulation is the dominant mechanism causing the conductance increase observed during functionalization. This is reasonable considering that NO_2 exposure is expected to alter

metal work functions.[20] Furthermore, this demonstrates that the functionalization technique can be used without dramatically changing the conductance of the nanotube if the Schottky barriers are protected adequately.

Once the functionalization and stabilization steps have been completed, the structure can be used as a scaffold for growing many other materials by ALD, including metals and their oxides, nitrides, and sulfides.[21] The diameters of the tubes can be set at any desired value because growth per ALD cycle is highly reproducible. By changing reactants after a certain number of ALD cycles, coaxial core−shell structures can also be constructed, as was seen in Figure 3e. If desired, hollow tubes of oxidation-resistant materials can be formed by removing the nanotube through oxidation.

In summary, a reliable technique for functionalizing suspended SWNTs for ALD applications has been developed. By using optimized functionalization parameters, the nanotubes can be coaxially coated with high-κ dielectric material that is exceptionally thin, continuous, and radially isotropic. Changes in nanotube conductance caused by functionalization can be minimized by Schottky barrier passivation. Because this technique avoids covalent modification, it is expected that the optoelectronic properties of the nanotubes are preserved. Applications of this functionalization technique include fabrication of SWNT devices with ultrathin gate dielectrics and coaxially gated geometries. This technique may also be used to coat SWNTs with hydrophilic material, potentially making them nontoxic.[22]

Acknowledgment. This work was supported in part by the National Science Foundation under grant CTS-0236584. A portion of the research presented here was carried out at the Center for Nanoscale Systems (CNS) at Harvard University.

References

(1) Javey, A.; Guo, J.; Farmer, D. B.; Wang, Q.; Yenilmez, E.; Gordon, R. G.; Lundstrom, M.; Dai, H. *Nano Lett.* **2004**, *4*, 1319−1322.

(2) Guo, J.; Goasguen, S.; Lundstrom, M.; Datta, S. *Appl. Phys. Lett.* **2002**, *81*, 1486−1488.

(3) Guo, J.; Lundstrom, M.; Datta, S. *Appl. Phys. Lett.* **2002**, *80*, 31923194.

(4) Hoenlein, W.; Kreupl, F.; Duesberg, G. S.; Graham, A. P.; Liebau, M.; Seidel, R. V.; Unger, E. *IEEE Trans. Compon. Packag. Technol.* **2004**, *27*, 629−634.

(5) Javey, A.; Kim, H.; Brink, M.; Wang, Q.; Ural, A.; Guo, J.; McIntyre, P.; McEuen, P.; Lundstrom, M.; Dai, H. *Nat. Mater.* **2002**, *1*, 241−246.

(6) Farmer, D. B.; Gordon, R. G. *Electrochem. Solid-State Lett.* **2005**, *8*, G89−G91.

(7) Bahr, J. L.; Tour, J. M. *Chem. Mater.* **2001**, *13*, 3823−3824.

(8) An, L.; Fu, Q.; Lu, C.; Liu, J. *J. Am. Chem. Soc.* **2004**, *126*, 10520−10521.

(9) Matero, R.; Rahtu, A.; Ritala, M.; Leskelä, M.; Sajavaara, T. *Thin Solid Films* **2000**, *368*, 1−7.

(10) Gosset, L. G.; Damlencourt, J.-F.; Renault, O.; Rouchon, D.; Holliger, Ph.; Ermolieff, A.; Trimaille, I.; Ganem, J.-J.; Martin, F.; Semeria, M.-N. *J. Non-Cryst. Solids* **2002**, *303*, 17−23.

(11) Lim, B. S.; Rahtu, A.; Gordon, R. G. *Nat. Mater.* **2003**, *2*, 749−754.

(12) Zheng, L. X.; O'Connell, M. J.; Doorn, S. K.; Liao, X. Z.; Zhao, Y. H.; Akhadov, E. A.; Hoffbauer, M. A.; Roop, B. J.; Jia, Q. X.; Dye, R. C.; Peterson, D. E.; Huang, S. M.; Liu, J.; Zhu, Y. T. *Nat. Mater.* **2004**, *3*, 673−676.

(13) Franklin, N. R.; Wang, Q.; Tombler, T. W.; Javey, A.; Shim, M.; Dai, H. *Appl. Phys. Lett.* **2002**, *81*, 913−915.

(14) Kong, J.; Franklin, N. R.; Zhou, C.; Chapline, M. G.; Peng, S.; Cho, K.; Dai, H. *Science* **2000**, *287*, 622−625.

(15) Peng, S.; Cho, K. *Nanotechnology* **2000**, *11*, 57−60.

(16) Seo, K.; Park, K. A.; Kim, C.; Han, S.; Kim, B.; Lee, Y. H. *J. Am. Chem. Soc.* **2005**, *127*, 15724−15729.

(17) Rogers, R. D.; Atwood, J. K. *J. Crystallogr. Spectrosc. Res.* **1984**, *14*, 1−11.

(18) Hausmann, D. M.; Kim, E.; Becker, J.; Gordon, R. G. *Chem. Mater.* **2002**, *14*, 4350−4358.

(19) Heinze, S.; Tersoff, J.; Martel, R.; Derycke, V.; Appenzeller, J.; Avouris, Ph. *Phys. Rev. Lett.* **2002**, *89*, 106801.

(20) Rodriguez, J. A. *Surf. Sci.* **1990**, *230*, 335−349.

(21) For a recent review of materials available by ALD, see Puurunen, R. *J. Appl. Phys.* **2005**, *97*, 121301.

(22) Sayes, C. M.; Liang, F.; Hudson, J. L.; Mendez, J.; Guo, W.; Beach, J. M.; Moore, V. C.; Doyle, C. D.; West, J. L.; Billups, W. E.; Ausman, K. D.; Colvin, V. L. *Toxicol. Lett.* **2005**, published online Oct. 17, dx.doi.org/10.1016/j.toxlet.2005.08.011.

NL052453D